ISSN 2963-7511
Journal of Engineering Researcher and Lecturer, Vol. 5, No. 1, 2026, pp. 30-43

Numerical and experimental performance evaluation of an Eppler 420–based horizontal-axis hydrokinetic turbine for low-velocity river applications

Ma. Leona Maye B. Pepito

Department of Mechanical Engineering, University of Science and Technology of Southern Philippines, **Philippines**

*Corresponding Author: leona.pepito@ustp.edu.ph

Received: 02 February 2026; *Revised*: 08 April 2026; *Accepted*: 14 April 2026

https://doi.org/10.58712/jerel.v5i1.202

Abstract: Small-scale hydrokinetic turbines offer a viable solution for harnessing renewable energy from low-velocity rivers and canals, particularly in developing countries such as the Philippines, where a large portion of hydropower potential remains untapped. However, limited studies have experimentally validated the performance of airfoil-based propeller hydrokinetic turbines optimized for shallow, low-speed water streams. This study addresses this gap by designing, simulating, fabricating, and experimentally evaluating a horizontal-axis propeller hydrokinetic turbine based on the Eppler 420 airfoil. A combined Computational Fluid Dynamics (CFD) and field-testing approach was employed to optimize blade geometry, tip speed ratio, and diffuser configuration for a turbine with a swept area of 0.18 m² operating at stream velocities of 0.7–1.3 m/s. CFD results indicate that the venturi-type diffuser increased the inlet water velocity by an average of 62%, resulting in a simulated shaft power increase from 56 W for the bare turbine to 70 W for the diffuser-augmented configuration. Field experiments conducted in a local river validated these trends, achieving a maximum measured shaft power of 65 W at 1.3 m/s with a corresponding power coefficient of approximately 0.30. The close agreement between simulated and experimental results confirms the suitability of the Eppler 420 airfoil for low-velocity hydrokinetic applications and demonstrates the effectiveness of diffuser augmentation. The findings provide practical design guidance and experimental validation for efficient small-scale hydrokinetic turbine deployment in shallow inland water streams.

Keywords: renewable energy; hydrokinetic turbine; Eppler 420; diffuser-augmented

1. Introduction

Hydrokinetic turbines, or free-flow water turbines, are considered one of the emerging renewable energy sources, alongside other renewables such as solar and wind energy, due to the predictability of flowing water in rivers and canals (Ileberi & Li, 2023; Kelvin Edem Bassey, 2023). The Philippines is experiencing increasing energy demand and strong economic growth and has excellent potential for hydropower development (Torrefranca et al., 2022). Figure 1 indicates that the country has a gross theoretical hydropower potential of 47,459 GWh/year, of which 20,334 GWh/year is technically feasible and 18,184 GWh/year is economically feasible. Despite this substantial resource base, only about 17% of the technically feasible potential has been developed, equivalent to approximately 3,457 GWh/year. In addition, a significant portion of existing hydropower capacity consists of aging units, with approximately 275 MW coming from installations that are over 40 years old. These figures highlight both the opportunity for expansion and the need for rehabilitation, particularly through decentralized river-based applications that can complement existing hydropower infrastructure.

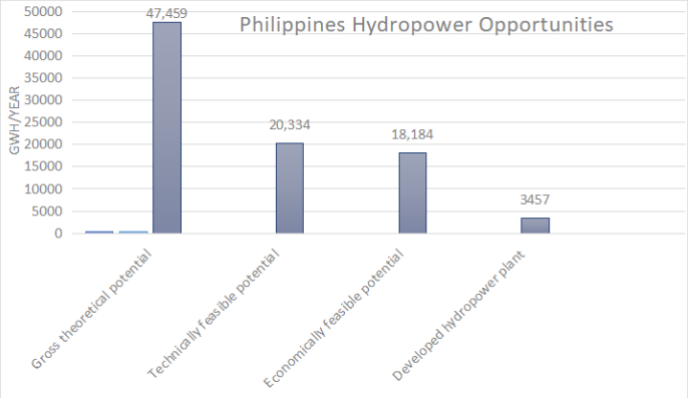

Figure 1. Philippines hydropower opportunities, Philippines: Country Profile (2019)

One of the main characteristics that distinguishes hydrokinetic technology from conventional hydroelectric plants is its environmental sustainability, as it does not require dams and its performance is not dependent on water head (Karalekas et al., 2013; Kelvin Edem Bassey, 2023). These turbines generate electricity by harnessing the kinetic energy of natural water flows using various types of rotors (Brasil Junior et al., 2019). The rotors are typically installed on fixed structures along riverbanks or on floating pontoons (Ibrahim et al., 2021; Saini & Saini, 2020). Most existing propeller blade profiles are primarily designed for wind turbines; however, they can also be adapted for hydrokinetic turbines. The hydrodynamic forces acting on hydrokinetic turbines are significantly greater than the aerodynamic forces on wind turbines due to the higher density of water compared to air. Therefore, it is essential to select a suitable blade profile that can withstand these higher loads. The performance of the E420 variant from Eppler airfoils, as investigated by Aguilar et al. (2019), shows promising results when used as a hydrofoil for water turbines compared to previous hydrofoil studies. However, this study was limited to CFD simulations focusing on the cross-sectional geometry under specified conditions. The proposed site has a depth of approximately 1.2 meters, a width of 1.5 meters, and an average flow velocity of 1.2 m/s.

The purpose of this study is to design, simulate, develop, and evaluate a horizontal-axis propeller turbine based on the Eppler 420 airfoil for local water stream applications. The study also aims to evaluate the optimum performance of the Eppler 420 propeller turbine with a swept area of 0.18 m². Simulation is conducted prior to prototyping to assess system behavior before fabrication.

2. Material and methods

The development phases in implementing the hydrokinetic system for local stream applications are shown in Figure 2. Hydrokinetic turbines are rotary devices that convert the energy of a moving stream of water into mechanical energy within the micro-hydro range for ultra-low head applications (Dincer & Ezzat, 2018). They are reaction-type turbines that utilize both velocity and pressure forces to generate power (Lamas Galdo et al., 2024; Ngcukayitobi, 2026). The design process of a hydrokinetic turbine system begins with site identification. The characteristics of the selected site at Pugaan River, Brgy. Sta. Ana, Tagoloan, Misamis Oriental serve as the basis for the hydrokinetic turbine design.

The design was preliminarily evaluated through Computational Fluid Dynamics (CFD) simulation using SolidWorks. To increase the efficiency of the designed propeller turbine, a diffuser-augmented housing was developed to focus the flow and enhance the inlet velocity. After obtaining the simulation results, the design was fabricated and tested at the selected site location.

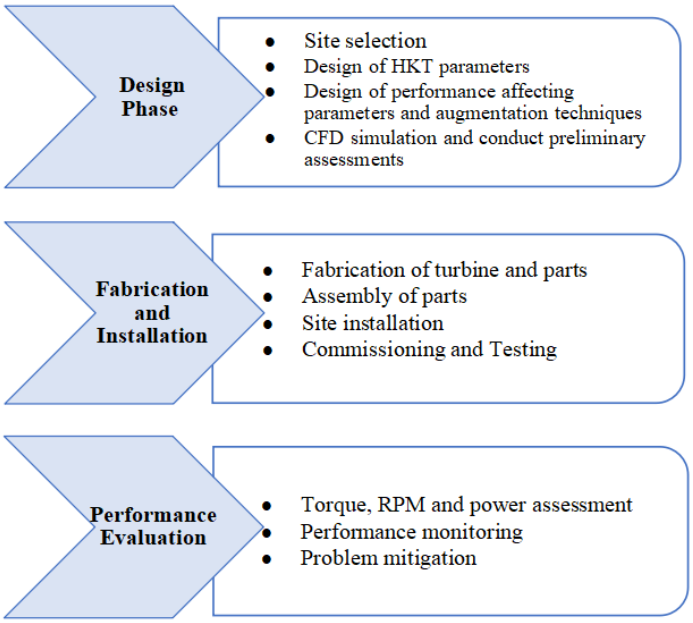

Figure 2. Development stages of the hydrokinetic system

2.1 Theoretical considerations

2.1.1 Tip Speed Ratio (TSR)

Tip speed ratio (TSR), denoted as λ, is a fundamental parameter in hydrokinetic turbine design. It represents the ratio between the blade tip speed and the incoming flow velocity. This parameter strongly influences turbine performance and efficiency (Puertas-Frías et al., 2022).

$$\lambda = \frac{\omega r}{v} \tag{1}$$

2.1.2 Relative velocity angle

The relative velocity angle (φ) defines the angle between the relative flow velocity and the rotor plane at a given blade section. Based on Blade Element Momentum (BEM) theory, this angle is derived from the velocity triangle formed by axial and tangential velocities (Puertas-Frías et al., 2022).

$$tan\ \emptyset = \frac{1-a}{\lambda r\ (1+ a'} \tag{2}$$

Under optimal design conditions (Betz-optimum approximation), this simplifies to:

$$\emptyset = \frac{2}{3}\tan^{-1}(\frac{1}{\lambda r}) \tag{3}$$

where φ is the relative velocity angle, λ is the tip speed ratio, and r is the local blade radius. This formulation is widely used in preliminary blade design for hydrokinetic and wind turbines.

2.1.3 Blade twist angle

The blade twist angle (β) is defined as the difference between the relative velocity angle and the design angle of attack. This ensures that each blade section operates at an optimal aerodynamic condition (Velásquez et al., 2025).

$$\beta = \emptyset - \alpha \tag{4}$$

where β is the blade twist angle, φ is the relative velocity angle, and α is the design angle of attack.

2.1.4 Chord length

Chord length (C) represents the width of the blade section and varies along the radius to maintain an optimal lift distribution. It is derived from BEM theory considering lift forces and flow conditions (Puertas-Frías et al., 2022).

$$C = \frac{8\pi r}{BC_l} \times 1 - \cos\emptyset \tag{5}$$

where C is chord length (m), r is blade radius (m), φ is the relative velocity angle, $C_l$is the lift coefficient, and B is the number of blades.

2.1.5 Buoyancy

Buoyancy is essential for maintaining the stability of hydrokinetic turbine systems, particularly floating configurations. It represents the upward force exerted by the fluid on a submerged body.

$$BF = \rho V g \tag{6}$$

where BF is buoyant force, ρ is fluid density (kg/m^3), V is submerged volume (m^3), and g is gravitational acceleration (m/s^2).

2.1.6 Torque

Torque (T) is generated by the tangential force acting on the rotor and is responsible for driving the generator shaft (Puertas-Frías et al., 2022).

$$T = Fr \tag{7}$$

where T is torque (N·m), F is tangential force (N), and r is blade radius (m).

2.1.7 Coefficient of torque

The coefficient of torque (C_t) evaluates the turbine's ability to extract rotational energy from the flow (Puertas-Frías et al., 2022).

$$C_t = \frac{T}{0.5\rho A r V^2} \tag{8}$$

2.1.8 Coefficient of power

The coefficient of power (C_p) represents the efficiency of converting kinetic energy into mechanical power.

$$C_p = C_t \lambda \tag{9}$$

2.1.9 Available power

The available power extracted from the flow is proportional to the cube of the flow velocity, indicating the strong dependence of turbine performance on flow conditions (Puertas-Frías et al., 2022).

$$P = \frac{1}{2}\rho A V^3 C_p \tag{10}$$

2.2 Design of propeller hydrokinetic turbine

2.2.1 Blade radius

The blade radius is directly related to the desired power output of the turbine. The blade radius can be determined through turbine sizing, which is based on the available power in the canal, the actual velocity of the water stream, and the efficiencies associated with electrical and mechanical losses in the turbine system. Using Eq. (9), the blade radius is calculated to be 0.2032 m.

2.2.2 Number of blades

Three blades were used for this propeller turbine. The reasons are mainly for higher efficiency and smoother output torque compared to a two-bladed turbine (Anyi & Kirke, 2011). Increasing the blades increases efficiency and smoother torque, but the cost of fabrication per blade must also be considered.

2.2.3 Propeller blade & hydrofoil selection

Most hydrofoils are originally derived from airfoils used in wind turbines; however, not all airfoils are suitable for hydrokinetic turbine applications. Based on the study by Aguilar et al. (2019) on the analysis of a lift-augmented hydrofoil for hydrokinetic turbines, the results showed that the E420 hydrofoil was identified as the most suitable profile due to its high lift performance at low stream velocities. In addition, its thicker profile enables it to withstand higher hydrodynamic loads during operation.

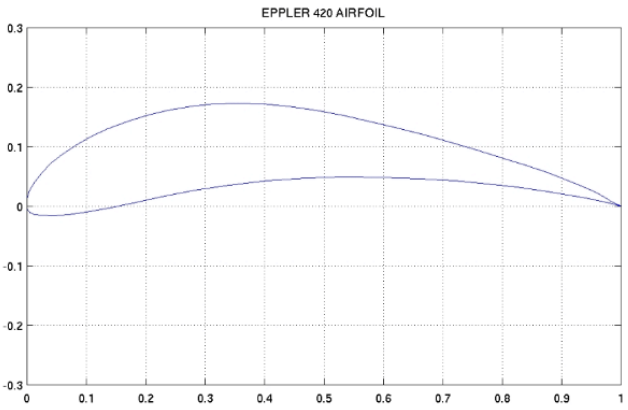

Figure 3. E420 airfoil plot (UIUC Airfoil Database)

To obtain accurate foil dimensions, the coordinates of the hydrofoil are presented in Figure 3. The curve data were processed using a Microsoft Excel spreadsheet. The optimum turbine blade, whether for wind or hydrokinetic energy extraction, is narrower at the tip and wider near the root (Anyi & Kirke, 2011). The blade is thicker at the root, where maximum flexural strength is required, and gradually becomes thinner toward the tip, where drag is minimized. The blade twist is significantly greater at the root than at the tip.

Table 1. Hydrofoil properties (Aguilar et al., 2019)

Parameter	Eppler 420 hydrofoil
Angle of attack (α)	3°
Lift coefficient (C_{l})	1.425
Drag coefficient (C_{d})	0.036

Before the chord length equation can be applied, the number of blades (B), lift coefficient (C_l), and relative velocity angle (ϕ) must first be determined. In this study, the number of blades used is three ($B = 3$). The lift coefficient (C_l) can be obtained from wind tunnel test data corresponding to the selected airfoil. Among the available airfoils that can be adapted as hydrofoils, the researchers selected the E420 airfoil from the Eppler airfoil family.

The relative velocity angle (ϕ) can be determined using Eq. (2); however, the design tip speed ratio (λ) must first be established. Since the blade radius is smaller than that of typical full-scale hydrokinetic turbines, a λ value of 3.2 was selected to achieve a thicker root and a narrower tip relative to the blade radius. The actual tip speed ratio can then be determined after the simulation process.

(a) (b)

Figure 4. Eppler 420 hydrofoil. (a) per plane and (b) Isometric view

Therefore, the values of B, C_l, ϕ, α, and λ have been determined, allowing the chord length (C) and blade twist angle (β) to be calculated for any radial position along the blade. The total blade length, which is 0.2032 m, is divided into 10 equal sections, as shown in Figure 4. Hence, each section is spaced at 20.32 mm intervals. The sections are represented as Plane No. 1 (r_1) to Plane No. 10 (r_{10}), where r_1 corresponds to the section nearest the root and r_{10} corresponds to the blade tip. The chord length increases from the tip toward the root. Similarly, the twist angle is larger near the root compared to the tip. The coordinates obtained for r_1 to r_{10} can be exported to SolidWorks software for precise, scaled printing, modeling, and simulation.

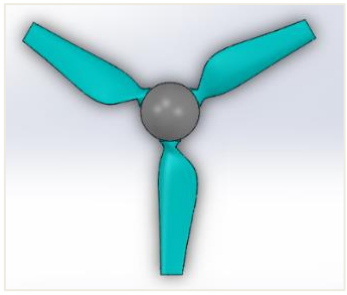

Figure 5. Propeller blade front view

2.2.4 Propeller hub

The hub illustrated in Figure 6 has an outer diameter of 88.9 mm (3.5 in), a bolt diameter of 6.35 mm (0.25 in), a blade hole diameter of 31.75 mm (1.25 in), a shaft hole diameter of 17 mm (0.67 in), and a height of 44.45 mm (1.75 in).

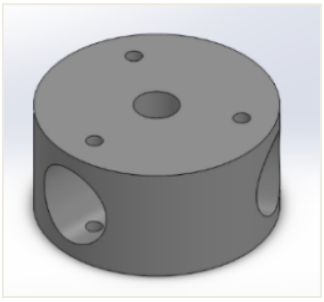

Figure 6. Propeller hub design

2.2.5 Nacelle

The nacelle consists of separable components, namely the head, body, and tail. The nacelle shown in Figure 7 is threaded and watertight, allowing the head and tail to be easily removed from the body. It is made of engineering plastic, and rubber O-rings are installed at the connection points to ensure sealing. The head houses the bearing assembly and can be removed independently without detaching the nacelle from the nacelle–diffuser assembly.

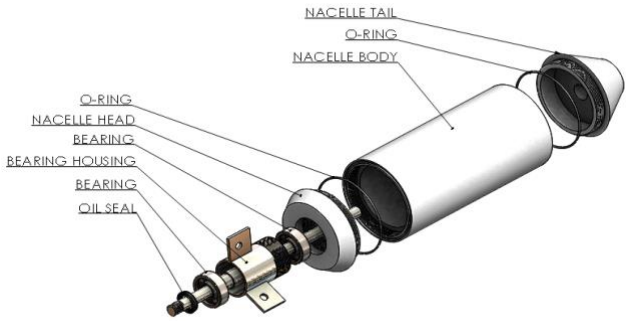

Figure 7. Nacelle assembly exploded view

2.2.6 Diffuser housing parameters

A diffuser, as illustrated in Figure 8, is typically used to increase the flow velocity entering the turbine, resulting in higher power output and improved system efficiency. The area ratio, as suggested by Riglin et al. (2014), ranges from 1.2 to 2, while the diffuser angle ranges from 5° to 15°. Gilbert & Foreman (1982) suggested that, for optimum performance, diffuser angles should exceed 6–8°. In addition, incorporating a shroud with a length-to-rotor diameter ratio of 0.5, and maintaining a clearance between the blade and the cover of approximately 3% of the rotor diameter, can further enhance performance efficiency due to more concentrated fluid flow.

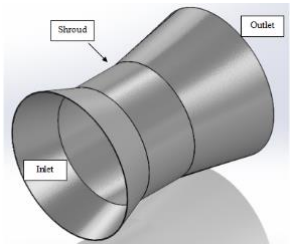

Figure 8. Venturi duct diffuser housing design

The venturi duct dimensions are summarized in Table 2, where the fluid pressure decreases as the flow passes through the constricted section in which the turbine blade is located, thereby allowing a greater volume of fluid to pass through at higher velocity.

Table 2. Geometric dimensions of the venturi duct housing

Parameters	Dimensions
Area ratio of diffuser	1.6
Diffuser angle inlet	18 degrees
Diffuser angle outlet	9 degrees
Diameter of shroud	0.497 m
Diameter of diffuser	0.628 m (inlet and outlet)
Length of shroud	0.249m
Total length of the housing	0.8 m

2.2.7 Floater assembly

The diffuser housing is supported by cylindrical floaters, as shown in Figure 9, each having a length of 1 m and a diameter of 4 in. The floaters are further supported by 1 in × 0.25 in angle bars, which serve as the structural frame connected to the housing.

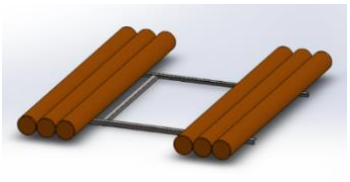

Figure 9. Floater

Designed to float and hold the entire mechanical device illustrated in Figure 10, on the surface of the water with enough buoyant force to ensure that it will not sink during the entire process.

(a) (b)

Figure 10. Propeller turbine design assembly (a) front view (b) side view

2.3 Computational Fluid Dynamics

The design was evaluated using SolidWorks Computational Fluid Dynamics (CFD) simulation prior to fabrication to facilitate the development of a functional full-scale prototype while minimizing performance deviations from the ideal optimized geometry of the Eppler 420 propeller blade with diffuser.

2.4 Development of the Eppler 420 propeller hydrokinetic turbine

The Eppler 420 propeller HKT blade was fabricated using WCL fiberglass and non-sag epoxy, which provide the blade edges with high strength-to-weight ratios and improved fatigue and corrosion resistance compared to other materials used in hydrokinetic turbines. The nacelle was manufactured by machining engineering plastic, as it is resistant to corrosion and lightweight. The integration of O-rings and oil seals, along with the application of epoxy putty to leakage-prone areas of the nacelle, helps ensure proper sealing and prevents flooding during operation. The Eppler 420 propeller HKT nacelle–blade assembly, as shown in Figure 11, was mounted on a venturi duct housing made of galvanized iron (GI) sheet, which was coated with primer and topcoat to prevent corrosion. For turbine installation, the Eppler 420 propeller HKT was mounted on a floating structure.

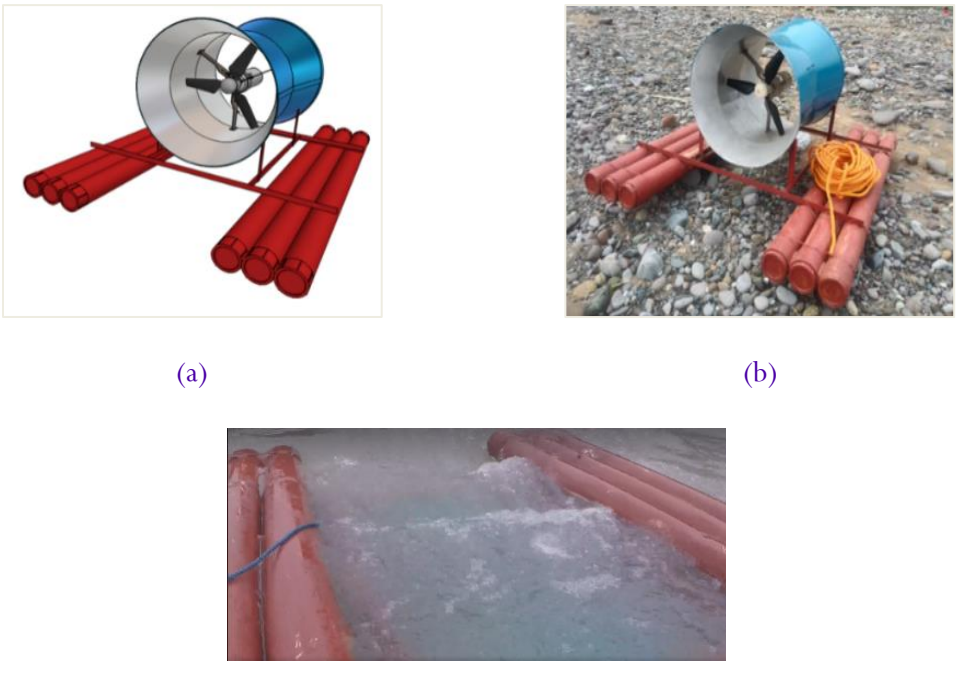

(a) (b)

(c)

Figure 11. Inverted HKT system. (a) SolidWorks model, (b) Actual set-up, and (c) Operating Eppler 420 HKT system

3. Results and discussion

Computational Fluid Dynamics (CFD) simulation analysis significantly contributes to the validation of theoretical design calculations, as the exact geometry is not easily reproducible in physical experiments. The design was evaluated through simulation to facilitate the development of a functional full-scale prototype while minimizing performance deviations from the ideal optimized geometry of the propeller blade with diffuser. This chapter presents the data and results obtained during the actual

testing of the developed horizontal-axis propeller hydrokinetic turbine using the Eppler 420 airfoil for local water stream applications. The experiments were conducted in October 2021, November 2021, December 2021, January 2022, and February 2022 at the Pugaan River, located in Brgy. Bontong, Sta. Ana, Misamis Oriental. The data were collected using a data logger, and the results were used to evaluate the performance of the developed horizontal-axis Eppler 420 propeller hydrokinetic turbine system.

4.1 Simulation results of the propeller hydrokinetic system

The assessment of the designed propeller hydrokinetic system, and flow simulation analysis for the venturi duct were conducted first to validate the increase in velocity throughout the system, shown in Figure 12. The inlet velocity was from 0.7 to 1.3 m/s which was based on the actual velocity tested in the local stream which is 1 m/s.

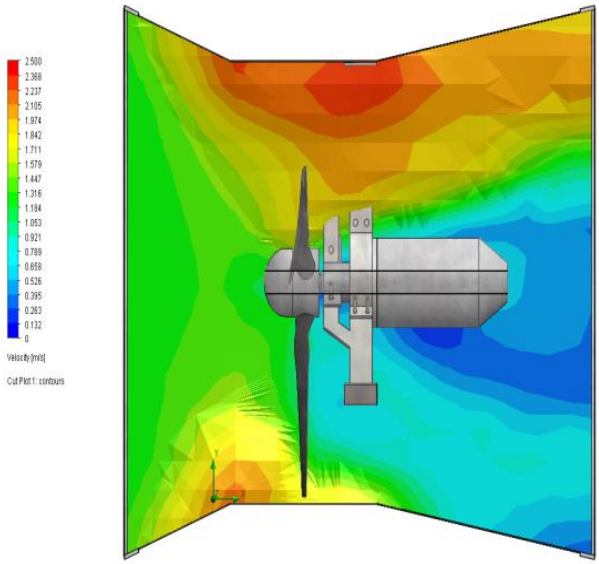

Figure 12. Velocity profile at various stream velocity

It shows an average of 62% increase in velocity as water passes through the venturi duct system. The evaluation based on SolidWorks showed that the designed 3-blade Propeller turbine increased the shaft power from 56 Watts for the bare turbine to 70 Watts for the diffuser augmented turbine. Also, it shows the velocity of water as it flows from right to left, and increases as it reaches the shroud, both upper and bottom flow reaching a peak the point where the inlet and the shroud coincide. It is noticeable that the maximum velocity was attained at the rear-end of the shroud, in which the pylon is attached to the diffuser. The evaluation based on SolidWorks showed that the designed 3-blade Propeller turbine increased the shaft power from 56 Watts for the bare turbine to 70 Watts for the diffuser augmented turbine.

4.2 Simulation Results of the propeller hydrokinetic system

The three curves shown in Figure 13, indicate similar trends, validating that as water velocity increases, the turbine's extracted power increases. The maximum recorded actual shaft power was 65 Watts at 1.3 m/s water velocity. Due to limitations in the fabrication and other factors affecting the system's performance, the actual result is slightly lower than the simulation and theoretical results.

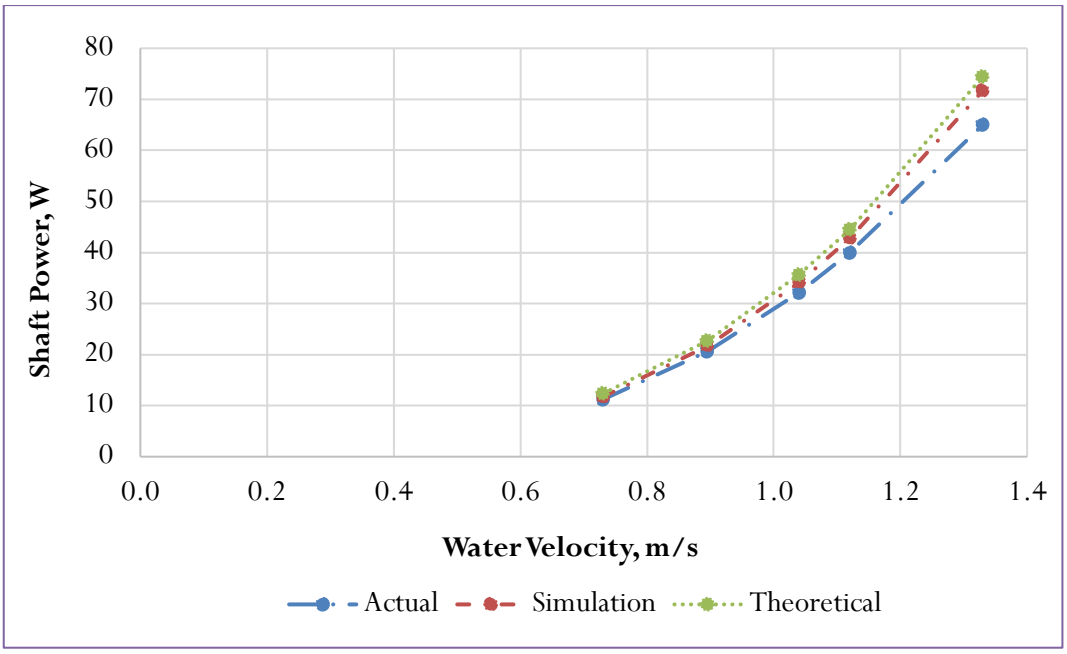

Figure 13. Eppler 420 HKT shaft power vs stream velocity

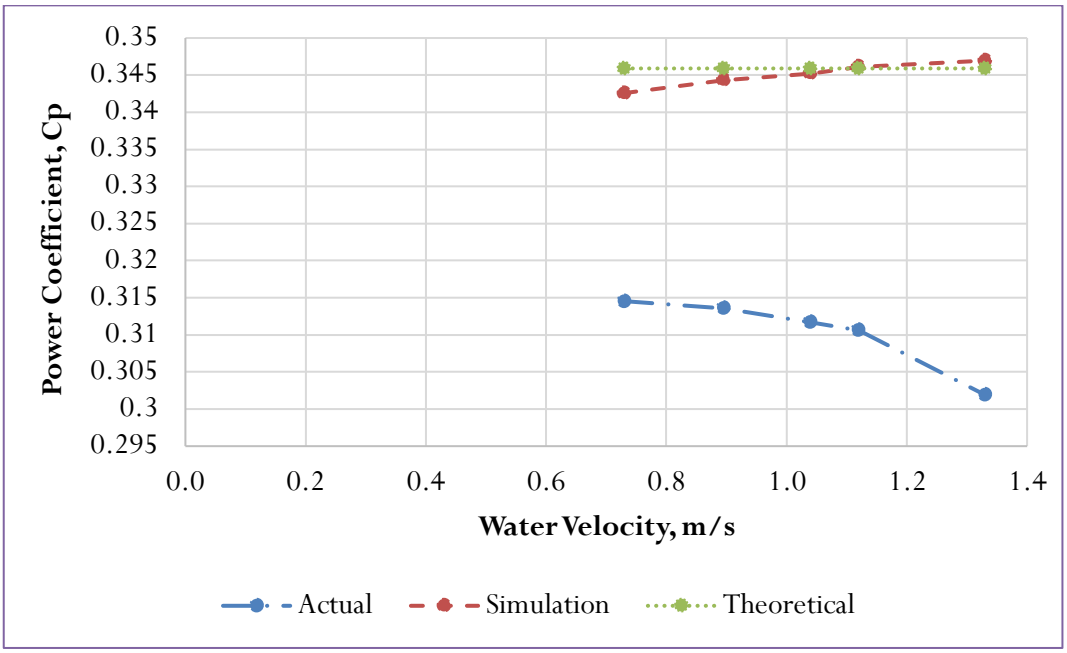

Figure 14. Eppler 420 HKT power coefficient vs stream velocity

The result shown in Figure 14 illustrates the close values for Simulated and Theoretical Power Coefficient, Cp against the stream velocity of around 0.35. On the other hand, the actual Cp based on the experimentation was around 0.31. This validates the optimum Cp as a function of design tip speed ratio (l=3.2) for a 3-bladed propeller turbine (Hazim et al., 2020). The performance of the E420 variation from Eppler airfoils which was used by Aguilar et al. (2019), shows promising results when it comes to using it as a hydrofoil for water turbines compared to previous hydrofoil studies which was limited to CFD simulation.

4. Conclusion

In the present study, a horizontal-axis propeller hydrokinetic turbine using the Eppler 420 air foil was designed and developed for local water stream applications. The performance of the turbine was evaluated experimentally at stream velocities ranging from 0.7 to 1.3 m/s in an open water channel. Based on the turbine performance, the river water velocity plays a significant role in maximizing the energy extraction potential of the turbine system. The venturi duct design for the propeller housing increased the incoming water velocity by 62%, thereby improving turbine performance. Furthermore, the floater assembly was able to safely support the turbine structure, and the materials used for the propeller and housing could withstand the forces generated by the incoming water flow. The evaluation using SolidWorks simulation showed that the designed three-blade propeller turbine increased the shaft power from 56 W for the bare turbine to 70 W for the diffuser-augmented turbine. Based on actual site experimentation, the Eppler 420 propeller turbine achieved a maximum shaft power of 65 W at a stream velocity of 1.3 m/s, with a power coefficient (C_p) of 0.3. This design is expected to contribute to the advancement of turbine design, modification, and performance analysis, as well as the development of hydropower components throughout the country.

Author's declaration

Funding statement

This research received no specific grant from any funding agency in the public, commercial, or not-for-profit sectors.

Data availability

The data that support the findings of this study are available from the corresponding author upon reasonable request. The data include CFD simulation outputs, experimental measurements, and processed performance results used in the analysis.

Acknowledgements

The author would like to acknowledge the support of the University of Science and Technology of Southern Philippines for providing facilities and technical assistance necessary for the completion of this study.

Conflict of interest

The authors declare that they have no known competing financial interests or personal relationships that could have appeared to influence the work reported in this paper.

Ethical clearance

Not Applicable.

AI statements

Grammarly was used to improve the grammatical structure of this article. The authors reviewed and verified the accuracy of the content, and an English language expert validated the data and language used.

Publisher's and Journal's Note

Researcher and Lecturer Society as the publisher, and the editor of Journal of Engineering Researcher and Lecturer state that there is no conflict of interest towards this article publication.

References

Aguilar, J., Rubio-Clemente, A., Velasquez, L., & Chica, E. (2019). Design and optimization of a multi-element hydrofoil for a horizontal-axis hydrokinetic turbine. *Energies*, *12*(24). https://doi.org/10.3390/en12244679

Anyi, M., & Kirke, B. (2011). Hydrokinetic turbine blades: Design and local construction techniques for remote communities. *Energy for Sustainable Development*, *15*(3). https://doi.org/10.1016/j.esd.2011.06.003

Brasil Junior, A. C. P., Mendes, R. C. F., Wirrig, T., Noguera, R., & Oliveira, T. F. (2019). On the design of propeller hydrokinetic turbines: the effect of the number of blades. *Journal of the Brazilian Society of Mechanical Sciences and Engineering*, *41*(6). https://doi.org/10.1007/s40430-019-1753-4

Dincer, I., & Ezzat, M. F. (2018). 3.4 Renewable Energy Production. In *Comprehensive Energy Systems* (pp. 126–207). Elsevier. https://doi.org/10.1016/B978-0-12-809597-3.00310-2

Gilbert, B. L., & Foreman, K. M. (1982). Experiments With a Diffuser-Augmented Model Wind Turbine. *American Society of Mechanical Engineers (Paper)*.

Hazim, S., El Ouatouati, A., Taha Janan, M., & Ghennioui, A. (2020). Performance of a hydrokinetic turbine using a theoretical approach. *Energy Reports*, *6*. https://doi.org/10.1016/j.egyr.2019.08.062

Ibrahim, W. I., Mohamed, M. R., Ismail, R. M. T. R., Leung, P. K., Xing, W. W., & Shah, A. A. (2021). Hydrokinetic energy harnessing technologies: A review. *Energy Reports*, *7*, 2021–2042. https://doi.org/10.1016/J.EGYR.2021.04.003

Ileberi, G. R., & Li, P. (2023). Integrating Hydrokinetic Energy into Hybrid Renewable Energy System: Optimal Design and Comparative Analysis. *Energies*, *16*(8). https://doi.org/10.3390/en16083403

Karalekas, P., Kowalski, G. J., & Lovelace, E. (2013). Modeling hydrokinetic turbine performance in the Mississippi river. *Marine Technology Society Journal*, *47*(4). https://doi.org/10.4031/MTSJ.47.4.21

Kelvin Edem Bassey. (2023). Hydrokinetic Energy Devices: Studying devices that generate power from flowing water without dams. *Engineering Science & Technology Journal*, *4*(2). https://doi.org/10.51594/estj.v4i2.1285

Lamas Galdo, M. I., Rodríguez García, J. de D., Couce Casanova, A., Blanco Damota, J., Caccia, C. G., Rebollido Lorenzo, J. M., & Telmo Miranda, J. (2024). Enhanced Performance of a Hydrokinetic Turbine through a Biomimetic Design. *Journal of Marine Science and Engineering*, *12*(8), 1312. https://doi.org/10.3390/jmse12081312

Ngcukayitobi, M. (2026). Comparative modelling of reaction and impulse turbines using ANN, ANFIS, and PSO-enhanced neural networks. *Discover Applied Sciences*, *8*(1). https://doi.org/10.1007/s42452-025-08100-z

Puertas-Frías, C. M., Willson, C. S., & García-Salaberri, P. A. (2022). Design and economic analysis of a hydrokinetic turbine for household applications. *Renewable Energy*, *199*. https://doi.org/10.1016/j.renene.2022.08.155

Riglin, J., Schleicher, W. C., & Oztekin, A. (2014). Diffuser optimization for a micro-hydrokinetic turbine. *ASME International Mechanical Engineering Congress and Exposition, Proceedings (IMECE)*, *7*. https://doi.org/10.1115/IMECE2014-37304

Saini, G., & Saini, R. P. (2020). Study of installations of hydrokinetic turbines and their environmental effects. *AIP Conference Proceedings*, *2273*. https://doi.org/10.1063/5.0024338

Torrefranca, I., Otadoy, R. E., & Tongco, A. (2022). Incorporating Landscape Dynamics in Small-Scale Hydropower Site Location Using a GIS and Spatial Analysis Tool: The Case of Bohol, Central Philippines. *Energies*, *15*(3). https://doi.org/10.3390/en15031130

Velásquez, L., Rengifo, J., Saldarriaga, A., Rubio-Clemente, A., & Chica, E. (2025). Optimization of Vertical-Axis Hydrokinetic Turbines: Study of Various Geometric Configurations Using the Response Surface Methodology and Multi-Criteria Decision Matrices. *Processes*, *13*(7). https://doi.org/10.3390/pr13071950